doi:10.1093/jmcb/mjab019
Published online March 24, 2021

Article

Cholesterol metabolic enzyme Ggpps regulates epicardium development and ventricular wall architecture integrity in mice

Feng Zheng[1,†], Zhong Chen[1,†], Qiao-Li Tang[1,†], Xin-Ying Wang[1], Dan-Yang Chong[1], Tong-Yu Zhang[1], Ya-Yun Gu[2], Zhi-Bin Hu[2,*], and Chao-Jun Li[1,2,*]

[1] Model Animal Research Centre, National Resource Centre for Mutant Mice, Medical School of Nanjing University, Nanjing 210093, China
[2] State Key Laboratory of Reproductive Medicine, Centre for Global Health, School of Public Health, Nanjing Medical University, Nanjing 211100, China
[†] These authors contributed equally to this work.
[*] Correspondence to: Chao-Jun Li, E-mail: licj@nju.edu.cn; Zhi-Bin Hu, E-mail: zhibin_hu@njmu.edu.cn

Edited by Anming Meng

During embryonic heart development, the progenitor cells in the epicardium would migrate and differentiate into noncardiomyocytes in myocardium and affect the integrity of ventricular wall, but the underlying mechanism has not been well studied. We have found that myocardium geranylgeranyl diphosphate synthase (Ggpps), a metabolic enzyme for cholesterol biosynthesis, is critical for cardiac cytoarchitecture remodelling during heart development. Here, we further reveal that epicardial Ggpps could also regulate ventricular wall architecture integrity. Epicardium-specific deletion of *Ggpps* before embryonic day 10.5 (E10.5) is embryonic lethal, whereas after E13.5 is survival but with defects in the epicardium and ventricular wall structure. *Ggpps* deficiency in the epicardium enhances the proliferation of epicardial cells and disrupts cell–cell contact, which makes epicardial cells easier to invade into ventricular wall. Thus, the fibroblast proliferation and coronary formation in myocardium were found enhanced that might disturb the coronary vasculature remodelling and ventricular wall integrity. These processes might be associated with the activation of YAP signalling, whose nuclear distribution is blocked by *Ggpps* deletion. In conclusion, our findings reveal a potential link between the cholesterol metabolism and heart epicardium and myocardium development in mammals, which might provide a new view of the cause for congenital heart diseases and potential therapeutic target in pathological cardiac conditions.

Keywords: geranylgeranylation, Ggpps, epicardial cells, cell connection, myocardium infarction

Introduction

The outer layer of the mammalian heart develops from the anterior epicardial layer of the venous pole adjacent to the cardiac tube at embryonic day 8.5 (E8.5) (Komiyama et al., 1987; Brade et al., 2013). The proepicardium, a cauliflower-shaped mass of coelomic cells that emerge from the pericardium close to the venous pole of the heart tube, protrudes toward the pericardial cavity during heart looping and finally develops into the epicardium (Perez-Pomares and de la Pompa, 2011). Epicardial cells are derived from *Nkx2.5*$^{+}$ and *Isl1*$^{+}$ cardiac progenitor cells and are specifically marked by transcription factor 21 (*Tcf21*), Wilms' tumour 1 (*Wt1*), and T-box18 (*Tbx18*) (Cai et al., 2008; Zhou et al., 2008a, b). Previous lineage-tracing studies in mouse embryonic hearts have shown that the outer epicardial cells could migrate into the ventricular wall structure and then differentiate into smooth muscle cells, vascular endothelial cells, cardiac fibroblasts, and even cardiomyocytes (Cai et al., 2008; Zhou et al., 2008a; Katz et al., 2012). During the embryonic period from E11.5 to E13.5, epicardial cells undergo a process called epithelial–mesenchymal transformation (EMT) to generate so-called epicardium-derived cells (EPDCs) (Brade et al., 2013). In postnatal mammals, this EMT process does not occur because the epicardial cells are in a quiescent physiological state (Zhou et al., 2011). However, under pathological conditions, such as myocardial infarction (MI), epicardial cells are reactivated, EMT is promoted, and cells go through similar developmental programmes to repair the injured adult heart (Zhou et al., 2011; Wei et al., 2015).

Received August 6, 2020. Revised December 9, 2020. Accepted December 21, 2020.

It is believed that the epicardium functions as a signalling centre that promotes the myocardial growth of the ventricular wall during embryonic development (Tian and Morrisey, 2012; Peralta et al., 2013; Plavicki et al., 2014). In our previous report, we found that a cholesterol synthesis enzyme of the mevalonate (MVA) pathway, geranylgeranyl diphosphate synthase (Ggpps), played an indispensable, stage-specific role in ventricular chamber maturation during mid-gestation (∼E12) by mediating protein geranylgeranylation of Rho GTPases (Chen et al., 2018). The MVA pathway is an important metabolic pathway for the synthesis of sterols and nonsteroidal isoprene in cells. The two downstream nonsteroidal isoprene products, farnesyl diphosphate (FPP) and geranylgeranyl diphosphate (GGPP), are important substrates involved in protein prenylation modification (McTaggart, 2006; Perez-Sala, 2007). Previous studies have shown that the MVA pathway is critical for heart tube formation in *Drosophila* and zebrafish (Yi et al., 2006; D'Amico et al., 2007). Our unpublished omics data also show that cholesterol biosynthesis was enhanced in the embryonic heart of mice. Using a genetic strategy of crossing *Nkx2.5-Cre* mice and floxed *Ggpps* mice, we generated cardiac progenitor cell-derived cardiomyocyte-specific *Ggpps* knockout mice, which cannot synthesize GGPP from FPP; we found that the knockout caused lethality at E12.5 by breaking cardiac cytoarchitecture during mid-gestation (Chen et al., 2018). We also found epicardial defects in *Ggpps*-deleted mice, as epicardial cells are also derived from Nkx2.5-positive cardiac progenitor cells.

To distinguish the effect of Ggpps in epicardial cells on epicardium formation and ventricular wall architecture integrity, we further constructed epicardial cell-specific *Ggpps*-deleted mice by crossing *WT1-Cre* mice and floxed *Ggpps* mice to exclude the effect of cardiomyocytes in the ventricular wall on the phenotype. We found that the epicardial *Ggpps*-deleted mice had a thicker epicardium structure, an abnormal ventricular wall with loose myocardial trabeculae, which might be associated with the hyperproliferation and morphology alteration of epicardial cells in the epicardium.

Results

Ggpps deletion in cardiomyocyte results in epicardial cell hyperproliferation and cardiomyocyte decline in the ventricular wall

We have found that cardiomyocyte-specific deletion of *Ggpps* using Nkx2.5-Cre could disrupt cardiac cytoarchitecture and result in embryonic lethality between E12.5 and E13.5 (Chen et al., 2018). Here, we also observed a thinner ventricular wall and loose myocardial tuberculum phenotype at E12.5 stage (Figure 1A). The mRNA and protein levels of WT1 in the heart examination indicated that WT1 was significantly upregulated at E12.5 after *Ggpps* deletion (Supplementary Figure S1A and B). This suggested that there were more epicardial cells at E11.5 and E12.5 after *Ggpps* knockout, which was confirmed by the existence of WT1-positive cells in the epithelium (Figure 1A; Supplementary Figure S1C). Meanwhile, cardiomyocyte number also declined in the compact layer of ventricular wall at E12.5 after *Ggpps* deletion, which was shown by cTnT staining (Figure 1A; Supplementary Figure S1D). We then performed double immunostaining for the cell proliferation markers Ki67 and WT1 to examine the cell proliferation of the epicardium. The results showed that, relative to control mice, there were more proliferated epicardial cells with Ki67 and WT1 double-staining signals in the epicardium at E11.5 and E12.5 (Figure 1B; Supplementary Figure S1E), which indicated the hyperproliferative ability of epicardial cells after *Ggpps* deletion. We also noticed that although the ventricular wall was thinner, there were WT1-positive cells in the compact layer of the ventricular wall (Figure 1A and B, arrowheads). Epicardial cells undergo EMT into the myocardium and generate EPDCs such as fibroblasts. Thus, we performed staining for the fibroblast marker vimentin and found that there were more vimentin-positive cells in the myocardium of *Ggpps*-deleted mice on E11.5 and E12.5 (Figure 1C; Supplementary Figure S1F). These observations indicated that cardiac deletion of *Ggpps* in all cardiomyocytes using Nkx2.5-Cre could result in developmental defects of both the epicardium and myocardium because of the overproliferation of epicardial cells and fibroblasts in ventricular wall.

Ggpps deletion in epicardial cells results in the damage to integrity of ventricular wall architecture

Since both cardiomyocytes and epicardial cells can be derived from Nkx2.5-positive cardiac progenitor cells, we further constructed epicardial cell-specific *Ggpps*-deleted mice by crossing floxed *Ggpps* mice with *Wt1-Cre^{ERT2}* mice that could deleted genes specifically in epicardial cells (Supplementary Figure S2A and B). This deletion could exclude the direct effect of ventricular cardiomyocytes on the epicardium formation and ventricular wall architecture integrity when we used *Nkx2.5-Cre* mice to delete *Ggpps* in all myocardia. When we deleted *Ggpps* at E10.5 by injecting tamoxifen into pregnant mice, the embryos with epicardial *Ggpps* deletion failed to survive after E14.5 (Figure 2A), but the embryos survived until delivery when the deletion occurred after E13.5 (Figure 2B). This stage-specific embryonic lethality phenotype is similar with *NkxKO* mice whose embryos died at E12.5 (Chen et al., 2018). Although the thickness of the ventricular wall was similar between *Wt1KO* and control mice, there were many hollow areas found in the ventricular wall of the myocardium of E13.5 hearts (Figure 2C, black arrows; Supplementary Figure S2C), and there were even invaginations at the surface of the ventricular wall (Figure 2D, white arrow; Supplementary Figure S2D). Like in *NkxKO* mice, we could find more WT1-positive cells existed in the compact zone of the myocardium in *Wt1KO* mice (Figure 2E, arrowheads; Supplementary Figure S2E). It was also similar that *Ggpps* deletion in epicardial cells resulted in increased fibroblasts in the compact zone of the myocardium (Figure 2F; Supplementary Figure S2F).

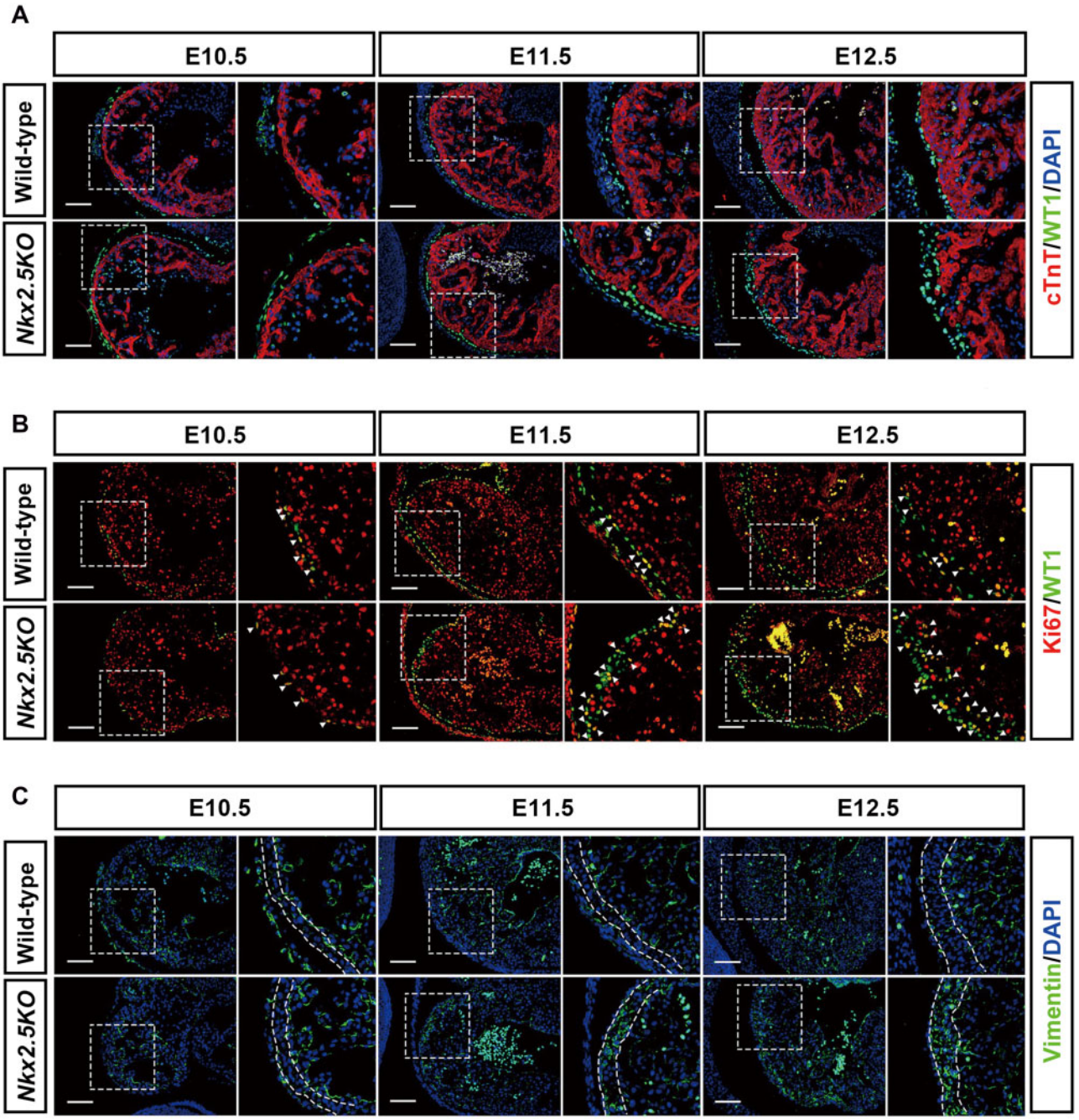

Figure 1 *Ggpps* deletion in cardiomyocytes results in epicardial cell hyperproliferation and fibroblast incline in the ventricular wall. (**A**) Immunofluorescence staining of WT1, cTnT, and DAPI in control and *Nkx2.5KO* hearts at E10.5, E11.5, and E12.5. Scale bar, 100 μm. (**B**) Immunofluorescence staining of Ki67 and WT1 indicates epicardial cell proliferation in control and *Nkx2.5KO* hearts at E10.5, E11.5, and E12.5. Scale bar, 100 μm. (**C**) Immunofluorescence staining of vimentin detects fibroblasts in control and *Nkx2.5KO* hearts at E10.5, E11.5, and E12.5. Scale bar, 100 μm.

Immunostaining of the endothelial marker PECAM further indicated that more vessel endothelial cells had formed after *Ggpps* deletion in epicardial cells (Figure 2G, arrows; Supplementary Figure S2G). This suggested that the formation of coronary vasculature might be augmented. All the above observations indicated that the deletion of *Ggpps* in epicardial cells might break the integrity of the myocardium because of the augmentation of vessel endothelial cells and fibroblasts.

Ggpps deficiency disrupts cell–cell contact of epicardial cells

We have shown that *Ggpps* deletion could break cell–cell junctions through inhibiting Rho GTPase prenylation and

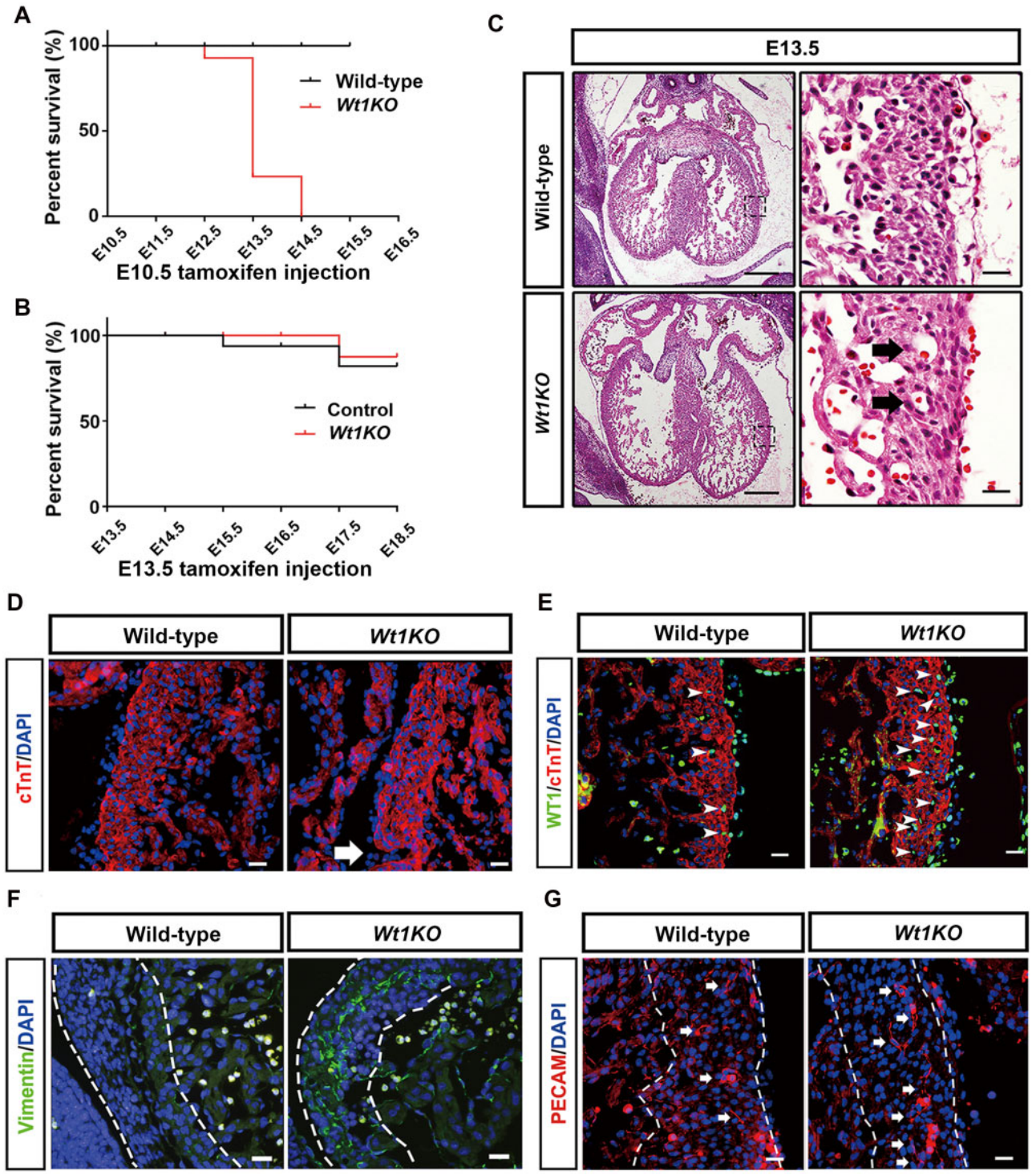

Figure 2 *Ggpps* deletion in epicardial cells results in the damage to ventricular wall architecture integrity. (**A**) Survival rate of *Wt1KO* mice when tamoxifen injected at E10.5. (**B**) Survival rate of *Wt1KO* mice when tamoxifen injected at E13.5. (**C**) Histology analysis of the epicardium in control and *Wt1KO* embryos at E13.5. Scale bar, 250 μm (left) and 50 μm (right). (**D**) Immunofluorescence staining of cTNT in the embryonic heart myocardium of *Wt1KO* and control mice. Scale bar, 50 μm. (**E**) Immunofluorescence staining of WT1, cTnT, and DAPI in the embryonic heart myocardium of *Wt1KO* and control mice. Scale bar, 50 μm. (**F**) Immu nofluorescence staining of vimentin and DAPI in the embryonic hearts of *Wt1KO* and control mice. Scale bar, 50 μm. (**G**) Immunofluorescence staining of PECAM and DAPI in the embryonic hearts of *Wt1KO* and control mice. Scale bar, 50 μm.

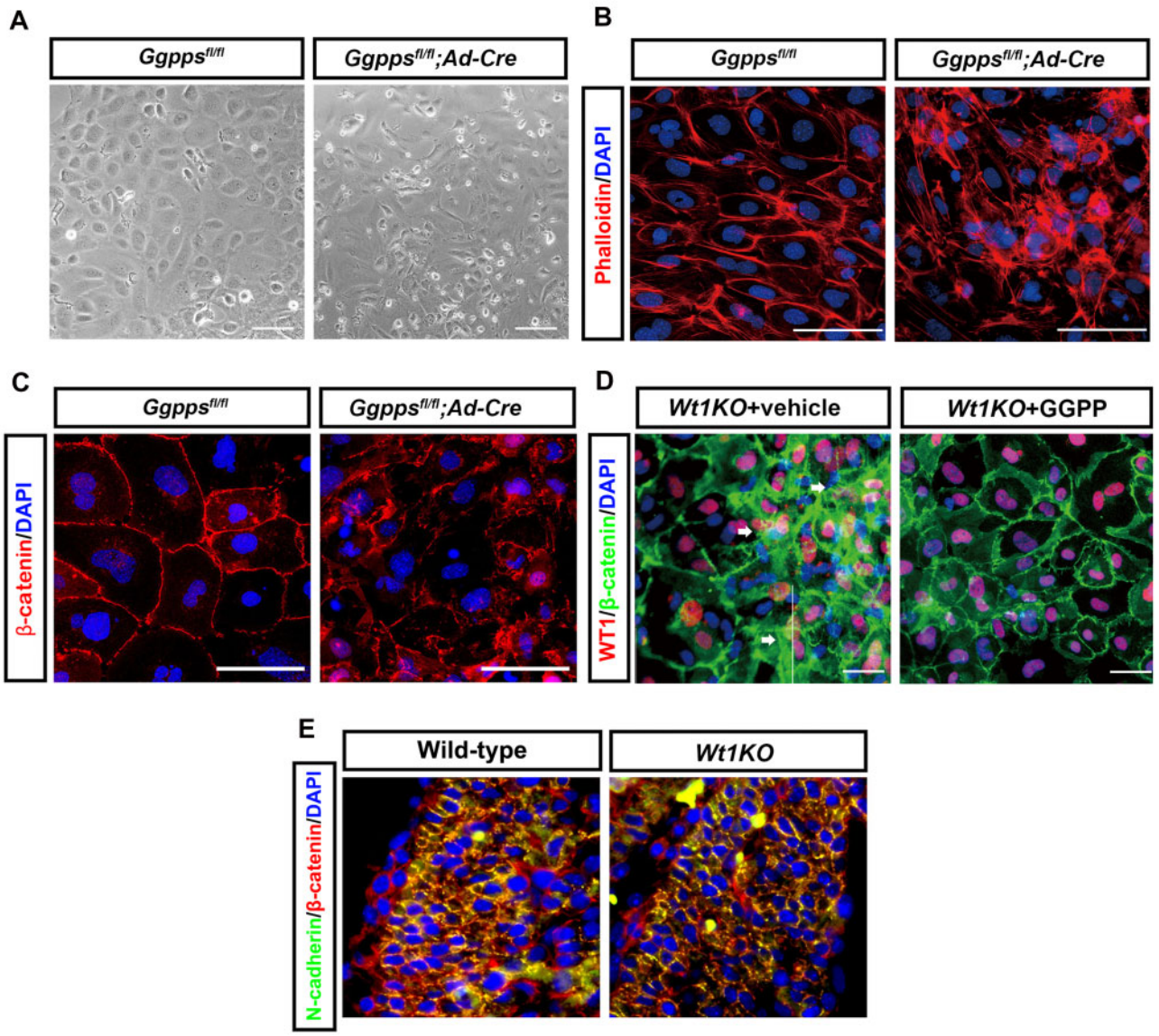

Figure 3 *Ggpps* deficiency disrupts cell–cell contact of epicardial cells. (**A**) Epicardial myocytes isolated from E13.5 hearts of floxed *Ggpps* mice were treated with a vehicle or Cre adenovirus. (**B**) Immunofluorescence staining of phalloidin and DAPI of the epicardial cells isolated from E13.5 hearts of floxed *Ggpps* mice. Scale bar, 50 μm. (**C**) Immunofluorescence staining of β-catenin and DAPI of the epicardial cells from E13.5 hearts of floxed *Ggpps* mice. Scale bar, 50 μm. (**D**) Immunofluorescence staining of WT1, β-catenin, and DAPI in the epicardial cells from *Wt1KO* embryonic hearts with vehicle or GGPP (20 μM) treatment. Scale bar, 50 μm. (**E**) Immunofluorescence staining of N-cadherin, β-catenin, and DAPI in the embryonic hearts of *Wt1KO* and control mice at E13.5. Scale bar, 50 μm.

then disrupt cardiac cytoarchitecture (Chen et al., 2018). To assess how Ggpps functions in epicardial cells, we isolated primary epicardial myocytes from E10.5–E13.5 hearts of floxed *Ggpps* mice and then infected them with Cre adenovirus to knock out *Ggpps in vitro*. The purity of the isolated cells was detected with WT1 immunostaining, and it showed that the majority of isolated cells were epicardial cells (>80%; Supplementary Figure S3). The morphology of epicardial cells was largely altered from flattened epithelial cells into irregular fibroblast forms (Figure 3A). The fluorescence staining of microfilaments with phalloidin indicated that the organization of microfilaments in the cytosol was also disordered in *Ggpps*-deleted epicardial cells (Figure 3B). Meanwhile, the cell–cell contact of epicardial cells was disrupted, as shown by accumulated cytosol location of β-catenin (Figure 3C). This chaotic situation of β-catenin could be recovered by the treatment of GGPP *in vitro* (Figure 3D). The rescue experiment also confirmed that the cell contact defect was really because of Ggpps-responsible GGPP formation. Immunostaining of N-cadherin and β-catenin in heart tissue also showed that cell–cell junction between cardiomyocytes in ventricular wall was disturbed in E13.5 *Wt1KO* mice (Figure

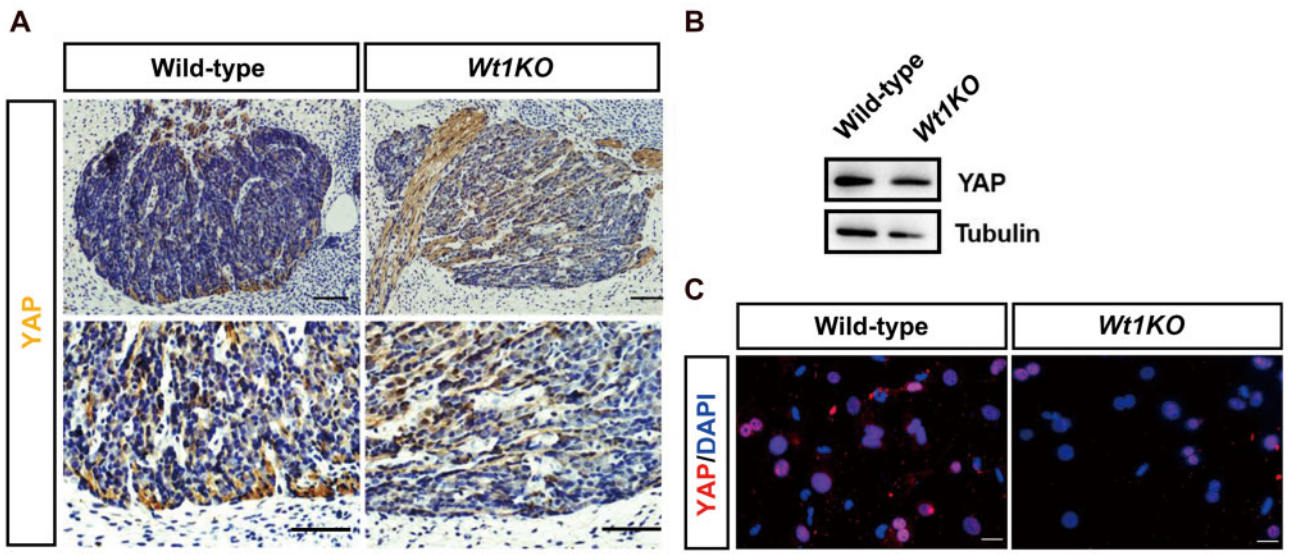

Figure 4 *Ggpps* deletion results in YAP inactivation. (**A**) Immunohistochemistry staining of YAP in the control ($n = 5$ for E13.5) and *Wt1KO* ($n = 6$ for E13.5) mice. Scale bar, 250 μm. (**B**) The protein expression of YAP in control and *Wt1KO* hearts was determined by western blotting analysis. $n = 6$. (**C**) Immunofluorescence staining of YAP in isolated epicardial cells from E13.5 control and *Wt1KO* mice. Scale bar, 50 μm.

3E). We could find more WT1-positive cells in the compact zone, because it was easier for them to invade into ventricular wall after *Ggpps* deletion. All the data suggest that *Ggpps* deficiency in the epicardium could disrupt cell–cell contact, and then epicardial cells would migrate into ventricular wall where they might differentiate to other EPDCs.

Ggpps deletion results in YAP inactivation

Ggpps can synthesize GGPP from FPP, and its deletion leads to a decrease in GGPP level and an inhibition of protein prenylation, such as Rho geranylgeranylation in cardiomyocytes (Bulhak et al., 2007). It has been reported that the Hippo/YAP signal could be regulated by protein prenylation through RhoA (Mi et al., 2015). It is also well known that Hippo/YAP are critical for the cellular response to mechanical force, and their expression significantly increases after ventricular chamber maturation (Zhao et al., 2011; Singh et al., 2016). Thus, we examined the expression of YAP in E13.5 embryonic hearts. YAP was found highly expressed in the compact zone of the myocardium and epicardium, whereas it was decreased in epicardial *Ggpps*-deleted mice (Figure 4A). The protein expression of YAP in total heart showed no statistical change between *Wt1KO* and the wild-type control (Figure 4B; Supplementary Figure S4A). However, when we isolated and cultured primary epicardial cells *in vitro*, we found that YAP was located in the nucleus of wild-type cells, but *Ggpps* knockout disrupted this nuclear location (Figure 4C; Supplementary Figure S4B). The results suggested that *Ggpps* deletion had an impact on nuclear location of YAP in epicardial cells during mouse embryonic heart development.

Ggpps deletion in the epicardium promotes MI recovery in adult mice

We also generated epicardial cell-specific *Ggpps*-deleted adult mice by injecting tamoxifen into 6-week-old mice. Through ligation of the left anterior descending branch of the mouse heart, MI was induced in these mice (Supplementary Figure S5A and B). Heart function examination indicated that there were not any cardiac defects in *Wt1KO* mice without heart injury (Figure 5A and B). Meanwhile, after MI challenge, the mild defect of the left ventricular diameter during diastole (LVIDD) or during systole (LVIDS) (Figure 5A–C) was observed in the *Wt1KO* mice. Although the survival curve of *Wt1KO* mice was prolonged (Supplementary Figure S5C), there was no significant difference of the ejection fraction and fraction shortening compared with that of the wild-type mice after MI (Supplementary Figure S5D and E). Meanwhile, the examination of fibrotic area indicated that there was also a tendency for better recovery from MI in the heart of *Ggpps*-deleted 6-week-old mice than wild-type mice (Figure 5D and E). The results suggested that inhibition of Ggpps may also have potential therapeutic effects under pathological cardiac conditions.

In conclusion, we have provided evidence that Ggpps-regulated epicardial cell proliferation is critical for heart development and heart function. *Ggpps* deletion during embryonic stage causes epicardial cells migrating into ventricular wall, where their hyperproliferation and differentiation would

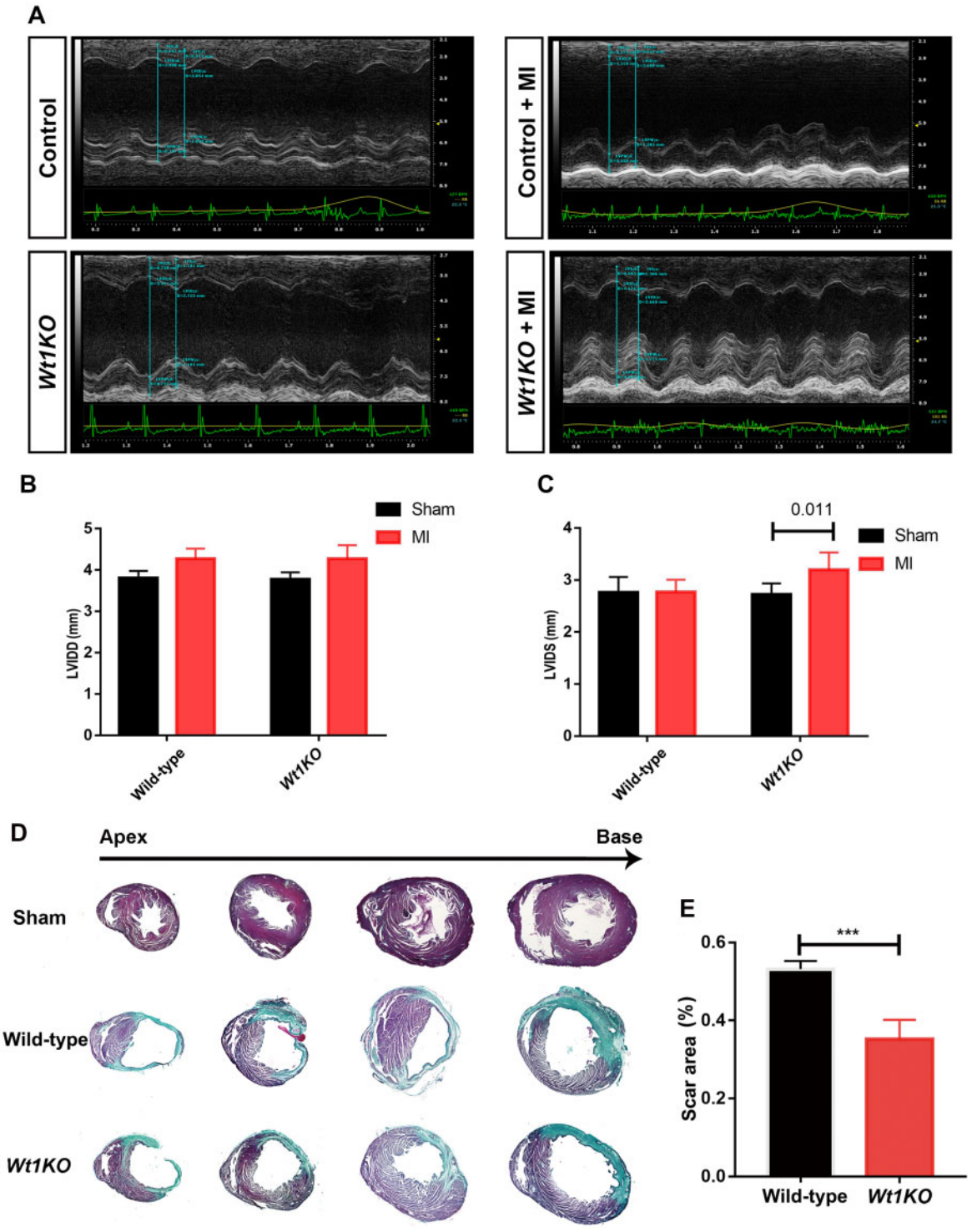

Figure 5 *Ggpps* deletion is beneficial to MI recovery in mice. (**A**) Cardiac function was examined with echocardiography of *Wt1KO* and control mice (left) and after 24 h with MI (right). (**B**) LVIDD in sham and MI groups of *Wt1KO* and control mice. (**C**) LVIDS in sham and MI groups of *Wt1KO* and control mice. During systolic stage, *Wt1KO* mice after MI show no difference with sham ($P = 0.011$). (**D**) Representative histological sections through multiple levels of the heart (apex toward base) with Masson's trichrome staining show the scar tissue in green and the healthy myocardium in red in wild-type and *Wt1KO* mouse hearts after MI. (**E**) The quantification of scar size in wild-type and *Wt1KO* mouse hearts after MI ($n = 6$, $^{***}P < 0.001$). Figures are representative of three independent experiments. Values are presented as mean ± SEM, with *P*-values by unpaired two-tailed Student's *t*-test.

damage the architecture integrity. On the contrary, these characteristics might be benefit to heart recovery after MI when *Ggpps* is deleted during adult stage.

Discussion

From E11.5 to E13.5, the epicardial cells undergo EMT process to differentiate into other cardiomyocytes such as fibroblasts and smooth muscle cells in ventricular wall (Komiyama et al., 1987; Cai et al., 2008; Brade et al., 2013). HMG-CoA reductase and other MVA pathway components like Ggpps could regulate the heart composition of *Drosophila* (Yi et al., 2006). We have reported that Ggpps-mediated protein geranylgeranylation plays an indispensable role as a stage-specific signal to regulate the establishment of chamber and cardiac cytoarchitecture around E12.5, in which the expression patterns and distribution of N-cadherin were disrupted by *Ggpps* deficiency in all cardiomyocytes (Chen et al., 2018). In the present study, we further detected the role of Ggpps in epicardial cells and found that Ggpps could also regulate the proliferation of epicardial cells and affect embryonic epicardium development and ventricular wall integrity.

Considering the incidence of hyperlipidemia and increased cholesterol levels during pregnancy, HMG-CoA reductase inhibitor statins are a potential but controversial therapeutic option for pregnant women (Nasioudis et al., 2019). Statins have been extensively used in the clinic as an effective treatment for hypercholesterolemia, but the strategies for applying these drugs appropriately in the clinic require more comprehensive studied during pregnancy. For example, statin could induce apoptosis that depends on a decrease in the membrane translocation of RhoA and Rac1 because of their prenylation inhibition (Dirks and Jones, 2006). An increase in intracellular Ca^{2+} levels caused by the loss of isoprene compounds may also activate mitochondrial-mediated apoptosis signalling pathways (Tomaszewski et al., 2011). Ggpps is an important enzyme that catalyses the synthesis of nonsterol isoprenoid GGPP from FPP (Goldstein and Brown, 1990). Both FPP and GGPP contribute to protein prenylation by farnesyl transferase and geranylgeranyl transferase, respectively, by conjugating lipid anchors to target proteins, which are essential for their association with and activation at the plasma membrane (Schafer and Rine, 1992). Isoprenylation by GGPP is crucial for the activation of small GTPases, such as Rho, Rac, and Cdc42, which are associated with various cellular functions, including gene expression and actin cytoskeleton remodelling (Braga et al., 1997; Jiang et al., 2006). Thus, protein prenylation was required in the early stages of heart development (Moses et al., 2001; Wessels and Perez-Pomares, 2004). In our previous study, cadherin-mediated adherin junctions were disrupted in *Nkx2.5-Ggpps* knockout heart in a Rho GTPase prenylation-dependent manner (Chen et al., 2018). Adherin junctions are also critical for cardiac trabeculation and trabecular regional specification (Ong et al., 1998; Cherian et al., 2016). The hyperproliferation of epicardial cells and fibroblasts in ventricular wall after *Ggpps* deletion would disrupt the cardiac trabeculation and trabecular regional specification, which has been reported to cause embryonic lethality or sudden arrhythmic death in adult (Kostetskii et al., 2005; Li et al., 2005).

The other reason that *Ggpps* deletion impairs heart development is the decrease of CoQ10. CoQ10 is an important coenzyme in the electron transport chain of the mitochondrial inner membrane, which is derived from GGPP (Quinzii et al., 2007). CoQ10 is most abundant in the heart compared with other organs. CoQ10 deficiency can also cause cardiomyopathy. Once *Ggpps* was deleted in epicardial cells, intracellular mitochondrial electron transport would be disrupted, resulting in abnormal cardiac function (Bentinger et al., 2007). Statins can also damage mitochondrial function by reducing the synthesis and content of CoQ10 in cardiomyocytes (Limongelli et al., 2012). Additional supplementation with CoQ10 may provide a potential treatment strategy for the clinical treatment of congenital heart failure due to the side effect of statin usage.

Compared with the control epicardium, a significant increase in the proliferation rate of *Wt1KO* epicardial cells was detected. Proliferation of epicardial cells is required for EMT, as epicardial cells undergoing cell-cycle arrest fail to invade the myocardium (Iismaa et al., 2018). Activated proliferation of epicardial cells in *Wt1KO* mice may contribute to accelerated EMT and subsequent migration of epicardial derivatives into the underlying myocardium.

The Hippo–YAP pathway is an evolutionarily conserved kinase cascade that functions in a context-dependent manner in cell fate determination, organ growth, tissue regeneration, and tumorigenesis (Zhao et al., 2011). Recent studies have implicated Hippo signalling in cardiac epicardium development and coronary vasculature formation. Hippo signalling components are required for coronary vasculature development and remodelling, and this signalling is vital for the expression of some epicardium-derived growth factors, including Fgf9, Raldh2, and Wnt5a (Singh et al., 2016). The nuclear translocation of YAP was regulated in RhoA prenylation-dependent manner (Chau et al., 2014) and thus *Ggpps* deletion would block these processes.

In summary, we provided evidence that Ggpps in epicardial cells mediates a stage-specific function that is involved in ventricular maturation and the establishment of epicardium structure. Our findings reveal a potential link between the MVA pathway inhibition by statins and heart development and congenital heart disease. GGPP administration might alleviate the side effect of statins to treat hyperlipidemia during pregnancy.

Materials and methods

Mice

Mice with floxed *Ggpps* (*Ggpps*$^{fl/fl}$) (Xu et al., 2015) were crossed with *Nkx2.5*$^{Cre/+}$ and *Wt1*$^{CreERT2/+}$ mice to generate *Nkx2.5*$^{Cre/+}$;*Ggpps*$^{fl/fl}$ and *Wt1*$^{CreERT2/+}$;*Ggpps*$^{fl/fl}$ mutants. The knockout of *Ggpps* was induced by injection of tamoxifen to

pregnant female mice and then the mice were sacrificed at the indicated time points via isoflurane inhalation followed by cervical dislocation. All mouse experiments conformed to the National Institutes of Health Guide for the Care and Use of Laboratory Animals and were carried out according to the protocol approved by the Animal Care and Use Committee of the Model Animal Research Centre of Nanjing University, Nanjing, China. All the control mice were born in the same litter of the knockout mice, and all mice were randomly selected from littermates.

Tamoxifen induction

For tamoxifen induction, tamoxifen (Sigma, T5648) was dissolved in ethanol and then was emulsified in sesame oil with sonication to a final concentration of 12.5 mg/ml. For the pregnant mice, tamoxifen was given (1 mg/10 g body weight) by gavage at the indicated time point to induce Cre expression. For adult mouse MI surgery, 4 mg tamoxifen was administered by gavage to 4- to 6-week-old mice twice weekly for 2 weeks.

Western blotting analysis

Total protein was extracted from frozen heart using NP40 buffer/RIPA containing a protease/phosphatase inhibitor cocktail. The protein concentration in each sample was determined using the BCA Protein Assay (Bio-Rad Laboratories). The same amount of protein (50 μg) was separated by 8%–12% sodium dodecyl sulphate–polyacrylamide gel electrophoresis, and resolved proteins were transferred to polyvinylidene fluoride membranes (Invitrogen) by standard methods. Immunoblots were blocked with 5% milk solution and incubated overnight at 4°C with primary antibodies against WT1 (Santa Cruz, sc-192, 1:100) and GAPDH (Kangchen Bio-tech, KC-5G4, 1:1000). Goat anti-rabbit or anti-mouse secondary antibodies (Kangchen Biotech, 1:5000) were used. Immunodetection was carried out using an enhanced chemiluminescence (ECL) kit (Tanon).

Total RNA isolation and quantitative polymerase chain reaction

Total RNA was isolated from embryonic hearts using TRIzol reagent (TaKaRa), and cDNA was synthesized with PrimeScript™ RT Master Mix (TaKaRa) according to the manufacturer's protocol. Quantitative polymerase chain reaction (PCR) was performed with SYBR™ Select Master Mix (Applied Biosystems) using an Applied Biosystems 7300 Real-Time PCR System. *Gapdh* was used as the internal control.

Histological analysis, immunohistochemistry, and immunofluorescence staining

Embryos from different developmental stages were collected and fixed in 4% paraformaldehyde (PFA) overnight. The sections were subjected to haematoxylin and eosin staining according to a standard protocol. For immunohistochemistry and immunofluorescence staining, deparaffinized and rehydrated paraffin sections were incubated with the indicated primary antibodies (1:200) at 4°C overnight: Ggpps (sc-271679, Santa Cruz), WT1 (sc-192, Santa Cruz), cTnT (MS-295-P0, Thermo Scientific), Ki67 (Ab15580 Abcam), vimentin (CL488-60330, Proteintech), β-catenin (610153, BD Biology), and YAP (D8H1X, Proteintech). Subsequently, the sections were incubated with secondary antibodies (1:200) for 1 h at room temperature: goat anti-rabbit IgG Alexa Fluor 594 (A11012), goat anti-mouse IgG Alexa Fluor 594 (A11032), goat anti-rabbit IgG Alexa Fluor 488 (A21206), and goat anti-mouse IgG Alexa Fluor 488 (A21202, Thermo Scientific).

Cell culture

Primary epicardial cells isolated from the hearts were maintained in serum-free DMEM (with 2 mM L-glutamine, 100 U/ml penicillin, and 100 U/ml streptomycin) under standard conditions. Briefly, E11.5–E12.5 mouse embryos were harvested, moved to a 6-well plate or Petri-dish with 1% gelatine, and pressed with sterile slides to make them adhere to the bottom to avoid floating. After 24 h of culture, the embryonic heart tissue was taken to continue the culture. The primary epicardial cells were maintained in DMEM with 10% volume fraction fetal bovine serum, 100 U/ml penicillin, and 100 U/ml streptomycin. After genotyping, control and *Ggpps*-deficient primary epicardial cells were treated with a vehicle or GGPP (Sigma, #G6025). Six embryos per group were used for cell culture.

MI model and triphenyltetrazolium chloride staining

Six-week-old male mice were used for MI surgery. After anaesthetized with 3% pentobarbital sodium (80 mg/kg), the mouse chest cavity was opened between the third and fourth ribs to fully expose the heart and the left anterior descending coronary artery or its area. The suture needle was inserted from the lower edge of the left atrial appendage to ligate the coronary artery. Then, the thoracic cavity and skin were completely sutured and closed. After naturally awakened, the mice were removed from the ventilator and reared normally.

For triphenyltetrazolium chloride (TTC) staining, MI hearts were quickly removed from the sacrificed mice, squeezed and rinsed with 4°C physiological saline to dip the blood contamination, and then frozen in the refrigerator at −20°C for 15 min until harden. The heart was cut into 1-mm-thick slices in the groove direction and quickly placed in TTC phosphate buffer (1%, pH 7.4) at 37°C water bath for 15 min. The infarct area is white after TTC staining, the infarct margin area is brick red, and the normal area is red.

Masson's trichrome staining

Paraffin tissue was dewaxed to water with different concentrations of alcohol and xylene. Haematoxylin staining, Ponceau staining, and Aniline blue staining were performed according to the Masson staining kit.

Data analysis

All data are presented as mean ± SEM, and analysis between two groups was performed using an unpaired two-tailed

Student's *t*-test. Multiple groups were tested by one-way analysis of variance followed by Bonferroni post hoc test. $*P < 0.05$ was considered as statistically significant. All statistical results were generated using Origin8.0 and GraphPad Prism7 software.

Supplementary material

Supplementary material is available at *Journal of Molecular Cell Biology* online.

Funding

This study was supported by the Key R&D Program of Jiangsu Province (BE2017708).

Conflict of interest: none declared.

References

Bentinger, M., Brismar, K., and Dallner, G. (2007). The antioxidant role of coenzyme Q. Mitochondrion *7(Suppl)*, S41–S50.

Brade, T., Pane, L.S., Moretti, A., et al. (2013). Embryonic heart progenitors and cardiogenesis. Cold Spring Harb. Perspect. Med. *3*, a013847.

Braga, V.M., Machesky, L.M., Hall, A., et al. (1997). The small GTPases Rho and Rac are required for the establishment of cadherin-dependent cell–cell contacts. J. Cell Biol. *137*, 1421–1431.

Bulhak, A., Roy, J., Hedin, U., et al. (2007). Cardioprotective effect of rosuvastatin in vivo is dependent on inhibition of geranylgeranyl pyrophosphate and altered RhoA membrane translocation. Am. J. Physiol. Heart Circ. Physiol. *292*, H3158–H3163.

Cai, C.L., Martin, J.C., Sun, Y., et al. (2008). A myocardial lineage derives from Tbx18 epicardial cells. Nature *454*, 104–108.

Chau, Y.Y., Bandiera, R., Serrels, A., et al. (2014). Visceral and subcutaneous fat have different origins and evidence supports a mesothelial source. Nat. Cell Biol. *16*, 367–375.

Chen, Z., Xu, N., Chong, D., et al. (2018). Geranylgeranyl pyrophosphate synthase facilitates the organization of cardiomyocytes during mid-gestation through modulating protein geranylgeranylation in mouse heart. Cardiovasc. Res. *114*, 965–978.

Cherian, A.V., Fukuda, R., Augustine, S.M., et al. (2016). N-cadherin relocalization during cardiac trabeculation. Proc. Natl Acad. Sci. USA *113*, 7569–7574.

D'Amico, L., Scott, I.C., Jungblut, B., et al. (2007). A mutation in zebrafish hmgcr1b reveals a role for isoprenoids in vertebrate heart-tube formation. Curr. Biol. *17*, 252–259.

Dirks, A.J., and Jones, K.M. (2006). Statin-induced apoptosis and skeletal myopathy. Am. J. Physiol. Cell Physiol. *291*, C1208–C1212.

Goldstein, J.L., and Brown, M.S. (1990). Regulation of the mevalonate pathway. Nature *343*, 425–430.

Iismaa, S.E., Li, M., Kesteven, S., et al. (2018). Cardiac hypertrophy limits infarct expansion after myocardial infarction in mice. Sci. Rep. *8*, 6114.

Jiang, H., Sha, S.H., and Schacht, J. (2006). Rac/Rho pathway regulates actin depolymerization induced by aminoglycoside antibiotics. J. Neurosci. Res. *83*, 1544–1551.

Katz, T.C., Singh, M.K., Degenhardt, K., et al. (2012). Distinct compartments of the proepicardial organ give rise to coronary vascular endothelial cells. Dev. Cell *22*, 639–650.

Komiyama, M., Ito, K., and Shimada, Y. (1987). Origin and development of the epicardium in the mouse embryo. Anat. Embryol. *176*, 183–189.

Kostetskii, I., Li, J., Xiong, Y., et al. (2005). Induced deletion of the N-cadherin gene in the heart leads to dissolution of the intercalated disc structure. Circ. Res. *96*, 346–354.

Li, J., Patel, V.V., Kostetskii, I., et al. (2005). Cardiac-specific loss of N-cadherin leads to alteration in connexins with conduction slowing and arrhythmogenesis. Circ. Res. *97*, 474–481.

Limongelli, G., Masarone, D., D'Alessandro, R., et al. (2012). Mitochondrial diseases and the heart: an overview of molecular basis, diagnosis, treatment and clinical course. Future Cardiol. *8*, 71–88.

McTaggart, S.J. (2006). Isoprenylated proteins. Cell. Mol. Life Sci. *63*, 255–267.

Mi, W., Lin, Q., Childress, C., et al. (2015). Geranylgeranylation signals to the Hippo pathway for breast cancer cell proliferation and migration. Oncogene *34*, 3095–3106.

Moses, K.A., DeMayo, F., Braun, R.M., et al. (2001). Embryonic expression of an Nkx2-5/Cre gene using ROSA26 reporter mice. Genesis *31*, 176–180.

Nasioudis, D., Doulaveris, G., and Kanninen, T.T. (2019). Dyslipidemia in pregnancy and maternal–fetal outcome. Minerva Ginecol. *71*, 155–162.

Ong, L.L., Kim, N., Mima, T., et al. (1998). Trabecular myocytes of the embryonic heart require N-cadherin for migratory unit identity. Dev. Biol. *193*, 1–9.

Peralta, M., Steed, E., Harlepp, S., et al. (2013). Heartbeat-driven pericardiac fluid forces contribute to epicardium morphogenesis. Curr. Biol. *23*, 1726–1735.

Perez-Pomares, J.M., and de la Pompa, J.L. (2011). Signaling during epicardium and coronary vessel development. Circ. Res. *109*, 1429–1442.

Perez-Sala, D. (2007). Protein isoprenylation in biology and disease: general overview and perspectives from studies with genetically engineered animals. Front. Biosci. *12*, 4456–4472.

Plavicki, J.S., Hofsteen, P., Yue, M.S., et al. (2014). Multiple modes of proepicardial cell migration require heartbeat. BMC Dev. Biol. *14*, 18.

Quinzii, C.M., Hirano, M., and DiMauro, S. (2007). CoQ10 deficiency diseases in adults. Mitochondrion *7(Suppl)*, S122–S126.

Schafer, W.R., and Rine, J. (1992). Protein prenylation: genes, enzymes, targets, and functions. Annu. Rev. Genet. *26*, 209–237.

Singh, A., Ramesh, S., Cibi, D.M., et al. (2016). Hippo signaling mediators Yap and Taz are required in the epicardium for coronary vasculature development. Cell Rep. *15*, 1384–1393.

Tian, Y., and Morrisey, E.E. (2012). Importance of myocyte–nonmyocyte interactions in cardiac development and disease. Circ. Res. *110*, 1023–1034.

Tomaszewski, M., Stepien, K.M., Tomaszewska, J., et al. (2011). Statin-induced myopathies. Pharmacol. Rep. *63*, 859–866.

Wei, K., Serpooshan, V., Hurtado, C., et al. (2015). Epicardial FSTL1 reconstitution regenerates the adult mammalian heart. Nature *525*, 479–485.

Wessels, A., and Perez-Pomares, J.M. (2004). The epicardium and epicardially derived cells (EPDCs) as cardiac stem cells. Anat. Rec. A Discov. Mol. Cell. Evol. Biol. *276*, 43–57.

Xu, N., Guan, S., Chen, Z., et al. (2015). The alteration of protein prenylation induces cardiomyocyte hypertrophy through Rheb–mTORC1 signalling and leads to chronic heart failure. J. Pathol. *235*, 672–685.

Yi, P., Han, Z., Li, X., et al. (2006). The mevalonate pathway controls heart formation in Drosophila by isoprenylation of Gγ1. Science *313*, 1301–1303.

Zhao, B., Tumaneng, K., and Guan, K.L. (2011). The Hippo pathway in organ size control, tissue regeneration and stem cell self-renewal. Nat. Cell Biol. *13*, 877–883.

Zhou, B., Honor, L.B., He, H., et al. (2011). Adult mouse epicardium modulates myocardial injury by secreting paracrine factors. J. Clin. Invest. *121*, 1894–1904.

Zhou, B., Ma, Q., Rajagopal, S., et al. (2008a). Epicardial progenitors contribute to the cardiomyocyte lineage in the developing heart. Nature *454*, 109–113.

Zhou, B., von Gise, A., Ma, Q., et al. (2008b). Nkx2-5- and Isl1-expressing cardiac progenitors contribute to proepicardium. Biochem. Biophys. Res. Commun. *375*, 450–453.